Journal of the Korean Physical Society, Vol. 45, December 2004, pp. S909∼S913

Two-Dimensional Quantum-Mechanical Modeling for Strained Silicon Channel of Double-Gate MOSFET

Kidong KIM,* Ohseob KWON, Jihyun SEO and Taeyoung WON
Department of Electrical Engineering, School of Engineering, Inha University, Incheon 402-751

S. BIRNER, R. OBERHUBER and A. TRELLAKIS
Physik-Department and Walter Schottky Institut,
Technische Universitat Munchen, D-85748 Garching

A novel structure of double-gate (DG) NMOSFET, which is formed by a strained silicon (Si) channel by using Si/$Si_{1-x}Ge_x$/Si, is proposed for the improvement of device characteristics. For analyzing the nano-scale DG MOSFET, a two-dimensional quantum-mechanical (QM) approach for solving the coupled Poisson-Schrödinger equations is reported. The advantages of a strained Si channel of DG MOSFET are discussed in terms of current drive, transconductance and mobility by varying the germanium concentration through our simulator. To analyze the short-channel effects of DG MOSFET, a subthreshold swing, a threshold voltage roll-off and the drain-induced barrier lowering were investigated. The difference in the calculated results between the classical and QM approaches is also demonstrated in this presentation.

PACS numbers: 85.30.De
Keywords: Strained silicon channel, Double-gate MOSFET, Quantum-mechanical simulation, Short-channel effects, Mobility enhancement

I. INTRODUCTION

As the CMOS scaling continues to shrink down at the nano-scale, there have been many efforts to improve the carrier mobility by employing a strained silicon (Si) channel. The strained Si channel comes from the 4.2 % lattice mismatch between Si and germanium (Ge). Through the reduced intervalley scattering and carrier-conductivity effective mass in tensile strained Si, the electron mobility is enhanced. Furthermore, the hole mobility is also enhanced, due to the alignment of band structure as well as the reduced in-plane effective mass in compressive strained Si [1,2]. Recently, a double-gate (DG) MOSFET structure has been considered as a promising candidate for sub-40 nm MOSFETs, due to its capability of scaling down characteristics, resistance against short-channel effects (SCE), high current drivability and suppression of drain field by two symmetric gates [3–6]. In order to optimize the structure of DG MOSFET, it is necessary to undertake a multi-dimensional quantum-mechanical (QM) simulation, because of the inherent quantum effects on the electronic properties of nano-scale semiconductor devices. To fulfill the numerical simulation of the nano-scale structures such as DG MOSFET, we need to obtain a self-consistent solution of the coupled Poisson-Schrödinger equations.

*E-mail: kkd@hsel.inha.ac.kr

In this paper, we report our QM modeling and simulation for the analysis of DG MOSFET in a self-consistent manner. Current-voltage (I-V) curves are demonstrated by varying the Ge concentration and gate length (L_g). Transconductance (G_m) of a strained Si channel is compared with the result for an unstrained Si channel. Electron-mobility enhancement, due to the reduction of intervalley scattering rates and carrier-conductivity effective mass is considered, both for a surface-channel and for a buried channel. SCE and quantum effects are also carefully investigated.

II. NUMERICAL MODEL

The two-dimensional (2-D) QM model is based on the self-consistent solution of coupled Poisson-Schrödinger equations to describe the effect of strain on the band structure of Si and bound states.

The 2-D QM model is based on the self-consistent solution of Poisson-Schrödinger equations in a simultaneous manner [7–9].

$$\bigtriangledown \cdot [\varepsilon(x,y) \bigtriangledown \Phi(x,y)] = -\rho(x,y), \quad (1)$$

$$\rho(x,y) = q[-n(x,y)+p(x,y)+N_D^+(x,y)-N_A^-(x,y)], \quad (2)$$

$$\{-\frac{\hbar^2}{2} \bigtriangledown \cdot M^\nu \bigtriangledown + V(x,y)\}\Psi_n(x,y) = E_n\Psi_n(x,y), \quad (3)$$

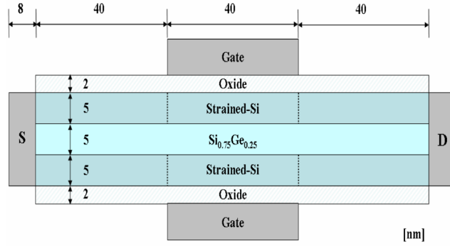

Fig. 1. Schematic diagram illustrating the structure of strained Si channel DG MOSFET.

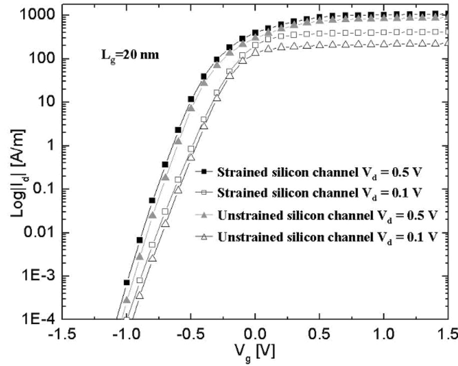

Fig. 2. Plot showing I_d-V_g curves for strained and unstrained Si channel DG MOSFET with L_g=20 nm.

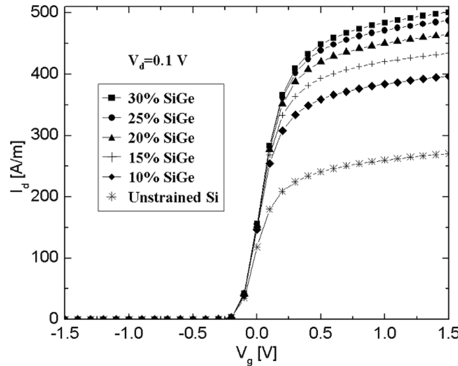

Fig. 3. Plot showing I_d-V_g curves at various Ge concentrations with L_g=40 nm.

where ε is the dielectric constant, Φ the electrostatic potential, ρ the total charge density, n and p the electron and hole concentrations, N_D^+ and N_A^- the ionized donor and acceptor concentrations, E_n and $\Psi_n(x,y)$ the energy and wave function of the nth eigenstate, $\hbar$ Planck's constant divided by 2π, the M^ν effective inverse mass tensor considering the six conduction valleys in Si, and V the potential energy, which is given by $V = \triangle E_c(x,y) - q\Phi(x,y)$. Here, $\triangle E_c(x,y)$ is the band offset in the conduction band.

For the solution of the Schrödinger equation, we used the mixed Dirichlet and von-Neumann boundary conditions which solve the Schrödinger equation with each condition respectively, and then normalized the states to 1/2. By solving the Schrödinger equation, we obtain the quantized states which are occupied with the local quasi-Fermi levels. The 2-D quantum electron density is found by using

$$n(x,y) = \frac{2}{\pi\hbar}\sum_{\nu=1}^{3}\sum_{n}\sqrt{2k_BT/M^\nu}|\Psi_n(x,y)|^2 \times F_{-1/2}(\frac{E_F - E_n}{k_BT}), \quad (4)$$

where E_F is the Fermi level and F_k the Fermi-Dirac integrals of order k. These integrals are defined as follows [7] :

$$F_k(\eta) = \frac{1}{\Gamma(k+1)}\int_0^\infty \frac{u^k du}{1+e^{u-\eta}}, \quad k \geq -1, \quad (5)$$

and also have the following property

$$\frac{dF_k(\eta)}{d\eta} = F_{k-1}(\eta), k \leq -1. \quad (6)$$

We obtain the semi-classical current solution from the 1st moment of the Boltzmann equation by adopting a simple drift-diffusion model for the electron current. It is as follows :

$$J_n(x,y) = \mu_n(x,y)n(x,y) \bigtriangledown E_{Fn}(x,y). \quad (7)$$

The continuity equation for current density is given by

$$\bigtriangledown \cdot J_n(x,y) = -R(x,y). \quad (8)$$

In order to obtain QM solutions, we have employed an iterative procedure. We start out by calculating the electric potential. Next, the program calculates a charge distribution by using an iteration scheme. Thereafter, the program determines self-consistent solutions of Poisson-Schrödinger and current equations [9]. The Newton method has been employed, with a constraint that should satisfy error criteria as outlined in [6].

Figure 1 schematically shows the strained Si channel DG MOSFET modeled in this work. Two metal gates with L_g and workfunction $\Phi_M = 4.1$ eV are located symmetrically on the top and the bottom of the device. The channel region is characterized by a $Si_{1-x}Ge_x$ layer between two strained Si layers. The source and drain regions are doped at 5×10^{19} /cm^3; the $Si_{1-x}Ge_x$ layer doping is 10^{14} /cm^3, and under the gate the doping is 10^{15} /cm^3. The oxide thickness (T_{ox}) is 2 nm, and L_g varies from 80 nm to 10 nm. We employed a finite difference method as a method of numerical analysis. As a test vehicle for verifying the validity of our numerical simulation, we chose an n-channel $Si/Si_{1-x}Ge_x/Si$ DG MOSFET, because of the good short-channel performance down to sub-10 nm MOSFET.

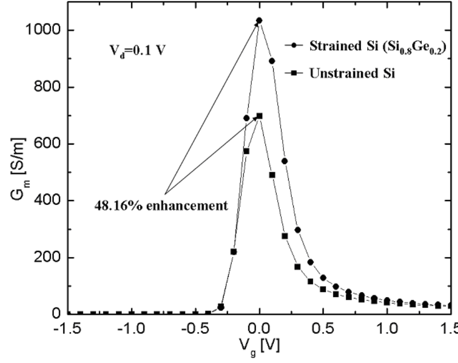

Fig. 4. Plot showing G_m for strained and unstrained Si.

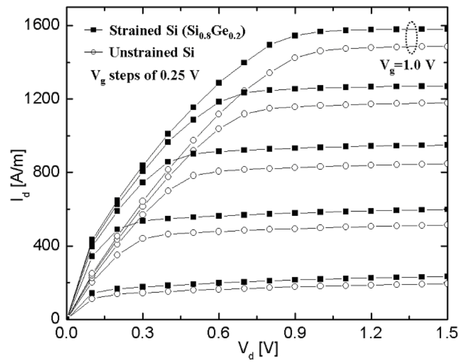

Fig. 5. Plot showing I_d-V_d curves for strained and unstrained Si channel DG MOSFET with L_g=40 nm.

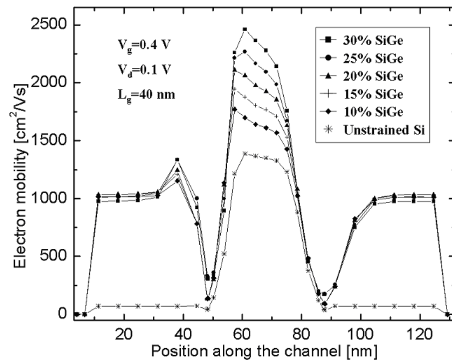

Fig. 6. Plot showing electron mobility of buried channel strained Si versus parallel position of channel at various Ge concentration.

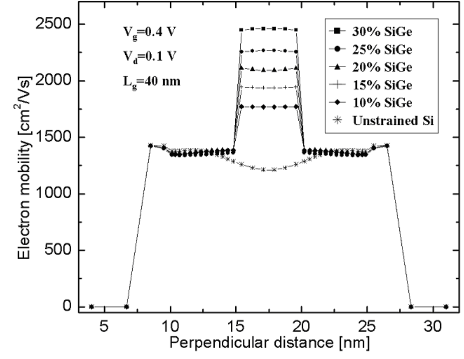

Fig. 7. Plot showing electron mobility of buried channel strained Si versus perpendicular position of channel at various Ge concentrations.

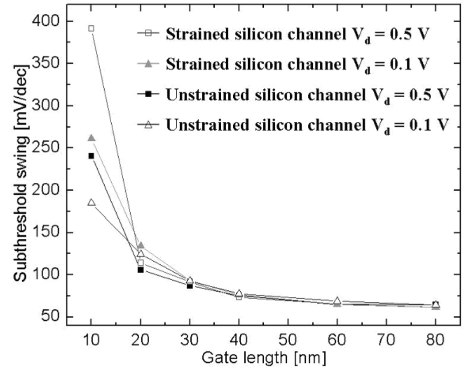

Fig. 8. Plot showing the subthreshold swing of DG MOSFET as a function of L_g.

III. SIMULATION RESULTS

In this work, we evaluated the mobility of strained channel DG MOSFET for surface and buried channel and investigated the SCE of strained and unstrained Si channel DG MOSFETs. Quantum effect at the Si/SiO_2 inversion layer is also studied from the difference in the results with and without QM effects being taken into account. Figure 2 shows the I_d-V_g characteristics of strained and unstrained channel DG MOSFET with L_g = 20 nm in a condition of V_d = 0.1 V and 0.5 V. The drain current in the strained Si channel is larger than the drain current for the unstrained Si channel, due to an enhanced mobility. Figure 3 shows I_d-V_g curves for various Ge concentrations. As the Ge concentration is increased, drain current is also increased because of the enhanced mobility. The enhancement of G_m for the strained and unstrained Si DG MOSFET is shown in Figure 4. We find that the G_m of the strained Si channel is 1033 S/m and is improved by 48 % compared to the unstrained Si channel. Figure 5 demonstrates the I_d-V_d characteristics for strained and unstrained Si channel DG MOSFETs. Here, the current in strained Si channels is increased compared to unstrained Si channels, due to the enhanced mobility.

The electron mobility in buried strained Si channels as a function of the parallel and perpendicular channel position is shown in Figures 6 and 7 for different Ge concentrations. Generally, the buried-channel strained Si MOSFETs exhibit very high performance compared to surface-channel strained Si in a limited voltage range. The mechanism of mobility enhancement in a strained Si channel is the reduction of intervalley scattering and carrier-conductivity effective mass in tensile strained Si. In the case of tensile strained Si, the 2-fold degenerate

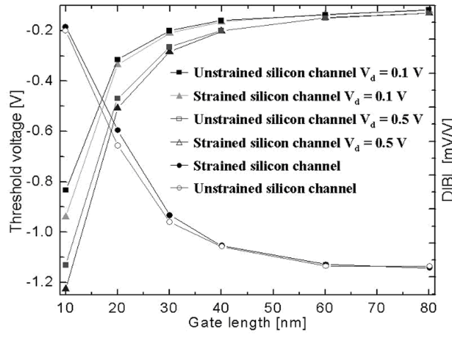

Fig. 9. Plot showing the Vt roll-off characteristic and drain-induced barrier lowering for DG MOSFET as a function of L_g.

valley is lower in energy and is occupied prior to the 4-fold degenerate valley. The conductivity effective mass m^* of all 6 valleys' contributions is as follows [2] :

$$\frac{1}{m^*} = \frac{1}{3}(\frac{1}{m_l} + \frac{1}{m_t}), \tag{9}$$

where m_l is the longitudinal mass and m_t is the transverse mass of the valley. Because the 2-fold degenerate valley dominantly contributes in tensile strained Si, only m_t is considered transverse to the direction of the channel. Consequently, the effective mass is given by

$$\frac{1}{m^*} = \frac{1}{m_t}. \tag{10}$$

Thus, the electron and hole mobility follow [2]

$$\mu = \frac{e\tau}{m^*}, \tag{11}$$

where e is the electronic charge and τ is the momentum relaxation time. Here, the mobility in the Si/SiO_2 inversion layer is relatively high, due to the electron confinement in the strained Si layer.

To analyze the short-channel effects, we extracted the parameters of subthreshold swing, threshold voltage (V_t) roll-off, and drain-induced barrier lowering (DIBL). Figure 8 demonstrates the subthreshold swings for an n-type DG MOSFET as a function of L_g in the conditions of strained and unstrained Si channel with V_d = 0.1 V and V_d = 0.5 V, respectively. In this work, we performed a numerical simulation under the condition of L_g varying from 10 nm to 80 nm, and this simulation gives results exhibiting good SCE. Figure 9 demonstrates the V_t roll-off characteristic and DIBL under the same conditions as Figure 8. The steepness of the V_t roll-off characteristic is similar in both strained and unstrained Si channel DG MOSFETs. The strength of DIBL is measured from the difference of V_t with variation of drain voltage to find the value of 10 mV/V and control the devices over the wide range of L_g [2]. These simulation results also show good SCE of DG MOSFET at smaller L_g.

Finally, we compared differences in the simulation results for classical and QM simulations. Figures 10(a),

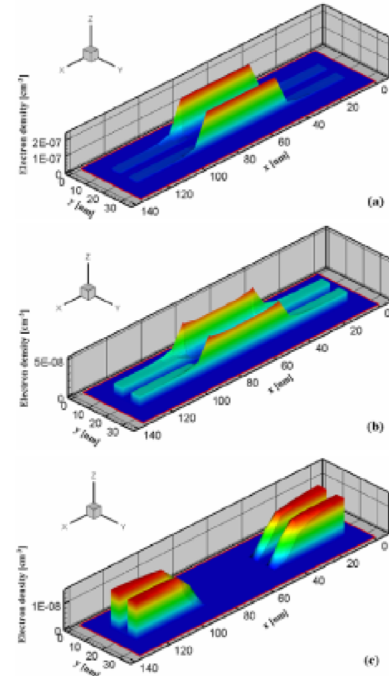

Fig. 10. Plot showing the electron densities of DG MOSFET with L_g = 40 nm, V_d = 0.1 V. (a) V_g = 1.5 V, (b) V_g = 0.5 V and (c) V_g = −1.5 V.

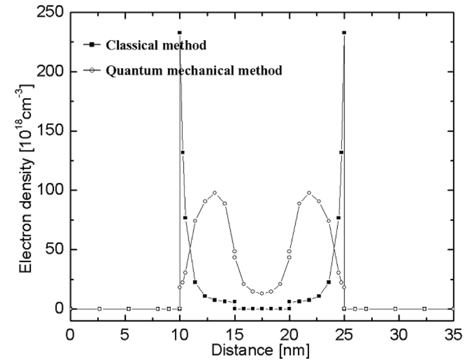

Fig. 11. Plot showing the comparison of the classical and QM electron density which is seen when cutting through the $Si/Si_{0.75}Ge_{0.25}/Si$ channel.

(b) and (c) demonstrate the distribution of electrons at several gate voltages : (a) V_g = 1.5 V, (b) V_g = 0.5 V and (c) V_g = −1.5 V. These figures show how the channels of DG MOSFET are formed, and the electron density is higher at S/D regions as the V_g decreases. A comparison of the classical and QM electron density as seen for a cut through the $Si/Si_{0.75}Ge_{0.25}/Si$ channel is shown in Figure 11. This result shows that the inclusion of QM size-quantization effects is crucial for the simulation of narrow channel structures, especially with respect to electron density near the oxide interface [10].

IV. CONCLUSION

In this paper, we have presented 2-D numerical modeling and simulation results with a self-consistent solution of the coupled Poisson-Schrödinger equations for a novel strained silicon (Si) channel double-gate (DG) MOSFET structure. It was revealed that the drain-current driving capability, as well as the transconductance, for the strained Si channel DG MOSFETs was tremendously improved when compared to the unstrained Si channels. The improvement in electron mobility has been investigated in terms of germanium concentration. Our simulation also revealed that short-channel effects could be appreciably suppressed for the DG MOSFET structure with respect to the influence of gate length. A significant difference in the electron density was observed for the quantum-mechanical simulation and the classical simulation, which implies that a full quantum mechanics is necessary for the correct analysis of sub-40 nm MOSFETs including the DG MOSFET employed in this work.

ACKNOWLEDGMENTS

This work was supported partly by the Korean Ministry of Information & Communication (MIC) through the Information Technology Research Center (ITRC) Program supervised by IITA, and partly by the Korean Ministry of Science and Technology (MOST) through KISTEP.

REFERENCES

[1] Karthik Chandrasekaran, Ph.D. Thesis, Nanyang Technological University, 2002.
[2] Sarah H. Olsen, Anthony G. O'Neill, Luke S. Driscoll, Kelvin S. K. Kwa, Sanatan Chattopadhyay, Andrew M. Waite, Yue T. Tang, Alan G. R. Evans, David J. Vorris, Anthony G. Cullis, Douglas J. Paul and David J. Robbins, IEEE Trans. Electron Devides. **50**, 1961 (2003).
[3] Zhibin Ren, Ramesh Venugopal, Supriyo Datta and Mark Lundstrom, Tech. Dig., International Electron Devices Meeting, (2001), p.107.
[4] H. R. Lee and H. S. Shin, J. Korean Phys. Soc. **44**, 56 (2004).
[5] A. Svizhenko, M. P. Anantram, T. R. Govindan and B. Biegel, J. Appl. Phys. **91**, 2343 (2002).
[6] S. E. Laux, A. Kumar and M. V. Fischetti, Tech. Dig., International Electron Devices Meeting, (2002), p.715.
[7] R. Akis, S. N. Milicic, D. K. Ferry and D. Vasileska, Intl. Conference on Modeling and Simulation of Microsystems, (2004), p.550.
[8] Y. S. Joe, J. Korean Phys. Soc. **26**, 536 (2004).
[9] M. Sabathil, S. Hackenbuchner, J. A. Majewski, G. Zandler and P. Vogl, J. Comp. Electronics. **1**, 81 (2002).
[10] S. H. Jin, Y. J. Park and H. S. Min, J. Korean Phys. Soc. **44**, 87 (2004).